

DETECTION OF AN IRON K EMISSION LINE FROM THE LINER NGC 4579

YUICHI TERASHIMA, HIDEYO KUNIEDA, AND KAZUTAMI MISAKI
Department of Physics, Nagoya University, Chikusa-ku, Nagoya 464-8602, Japan

AND

RICHARD F. MUSHOTZKY, ANDREW F. PTAK,¹ AND GAIL A. REICHERT
Laboratory for High Energy Astrophysics, Code 662, NASA/Goddard Space Flight Center, Greenbelt, MD 20771

Received 1997 December 1; accepted 1998 March 20

ABSTRACT

We present the results of an *ASCA* observation of the LINER NGC 4579. A pointlike X-ray source is detected at the nucleus with a 2–10 keV luminosity of 1.5×10^{41} ergs s^{-1} assuming a distance of 16.8 Mpc. The X-ray spectrum is represented by a combination of a power law with a photon index of ~ 1.7 and a soft thermal component with $kT \sim 0.9$ keV. An iron K emission line is detected at 6.73 ± 0.13 keV (rest-frame) with an equivalent width of 490^{+180}_{-190} eV, and it is statistically significant at greater than 99.9% confidence. The line center energy is consistent with helium-like iron and is significantly higher than 6.4 keV, which is expected from fluorescence by “cold” (or a lower ionization state of) iron. The iron line profile shows no significant red tail in contrast to Seyfert 1 galaxies, although the statistics are limited. The line center energy, the equivalent width, and the profile are consistent with an origin in an ionized accretion disk. However, the large mass accretion rate necessary to ionize the accretion disk is not consistent with the observed luminosity and the normal accretion models.

Subject headings: galaxies: individual (NGC 4579) — galaxies: nuclei — X-rays: galaxies

1. INTRODUCTION

Recent optical spectroscopic surveys have shown that there are many active galactic nuclei (AGNs) in nearby galaxies, and about 40% of bright galaxies are classified as Seyfert galaxies or LINERs (low ionization nuclear emission-line regions; Heckman 1980) (Ho, Filippenko, & Sargent 1997a). The luminosity of these objects is rather low compared to previously known AGNs, with a median value of the $H\alpha$ luminosity being only 2×10^{39} ergs s^{-1} in the sample of Ho et al. (1997a). Such objects (low-luminosity AGNs, hereafter LLAGNs) are important for investigating the physics of AGNs under an extreme condition, i.e., very low luminosity. X-ray observations probe the innermost regions of AGNs, and specifically, the iron K line provides information on the ionization state, the density, and the motion of matter very close to the central energy source.

ASCA observations of Seyfert 1 galaxies revealed that as a class, these objects have a broad iron K line with a profile skewed to lower energies, which is thought to be caused by the reprocessing of the continuum by a relativistic accretion disk (e.g., Tanaka et al. 1995; Nandra et al. 1997a). The center energy of the iron line from Seyfert 1 galaxies is consistent with 6.4 keV, which is expected from fluorescence by neutral or lower ionization states of (less than Fe xvi) iron in a disk with an inclination of less than 30° . In the Seyfert 1.9 galaxy IRAS 18325–5926, a higher peak energy of iron emission is seen that is compatible with a highly inclined disk ($i = 40^\circ$ – 50°) origin (Iwasawa et al. 1996). Highly ionized iron emission lines are detected from several radio-quiet quasars, e.g., E1821+643 (Kii et al. 1991; Yamashita et al. 1997) and PG 1116+215 (Nandra et al. 1996). Nandra et al. (1997b) studied the luminosity dependence of the iron line profile in a large sample of AGNs and found that the center energy increases and the red tail becomes weaker with increasing luminosity. They attrib-

uted such behavior to an increasing ionization of the accretion disk with increasing luminosity. Thus, X-ray measurements of iron emission lines are powerful diagnostic tools of matter in the vicinity of the nucleus.

There are only a few observations of iron emission lines from LLAGNs [L_X (2–10 keV) $\sim 10^{40}$ – 10^{41} ergs s^{-1}]. M81 (NGC 3031), with an X-ray luminosity of L_X (2–10 keV) $\sim 2 \times 10^{40}$ ergs s^{-1} , shows a broad iron line centered at ~ 6.7 keV with an equivalent width of ~ 200 eV. This line center energy is significantly higher than Seyfert 1 galaxies and similar to luminous quasars. An iron line at 6.4 keV with an equivalent width of ~ 300 eV is detected from the low-luminosity Seyfert 1 galaxy NGC 5033 [L_X (2–10 keV) $= 2 \times 10^{41}$ ergs s^{-1} ; Terashima et al. 1998b], but only an upper limit on the equivalent width of $\lesssim 300$ eV is obtained for NGC 1097 [L_X (2–10 keV) $= 1 \times 10^{41}$ ergs s^{-1} ; Iyomoto et al. 1996]. Although strong iron emission lines are also detected from M51 (=NGC 5194) (Terashima et al. 1998a), NGC 1365, and NGC 1386 (Iyomoto et al. 1997), the iron lines in these objects are interpreted as being caused by reprocessed emission from an obscuring torus and/or an extended ionized scatterer outside of our line of sight, i.e., these nuclei are heavily obscured. Thus, at present, the number of LLAGNs with small intrinsic absorption from which iron lines are detected is rather limited.

NGC 4579 (M58) is a Sab galaxy in the Virgo Cluster of galaxies and classified as a LINER or Seyfert 1.9 galaxy based on the optical emission lines (Ho et al. 1997a; Keel 1983; Stauffer 1982) and the broad $H\alpha$ component, detected with a FWHM of ~ 2300 km s^{-1} (Ho et al. 1997b). There exists a flat-spectrum radio core (Hummel et al. 1987). An *Einstein* HRI observation showed the presence of an unresolved X-ray nucleus, and the X-ray flux was measured to be $F_X = 7.9 \times 10^{-12}$ ergs s^{-1} cm^{-2} in the 0.2–4.0 keV band with the *Einstein* IPC (Fabbiano, Kim, & Trinchieri 1992; Halpern & Steiner 1983), which corresponds to the X-ray luminosity of 2.7×10^{41} ergs s^{-1} (we assume a distance of

¹ Present address: Department of Physics, Carnegie Mellon University, 5000 Forbes Avenue, Pittsburgh, PA 15213.

16.8 Mpc [Tully 1988] throughout this paper). These facts indicate the presence of a LLAGN in this galaxy. A recent ultraviolet imaging observation by the *Hubble Space Telescope* (*HST*) Faint Object Camera (FOC) detected a point source at the nucleus (Maoz et al. 1995). Its UV spectra were taken by the *HST* Faint Object Spectrograph (FOS), and a featureless UV continuum is detected as well as various emission lines. Comparison of the FOC and FOS data also indicate a factor of 3.3 decrease of UV flux in 19 months. The narrow UV emission lines are incompatible with the shock excitation model, and a photoionization model is preferred (Barth et al. 1996). Several broad UV emission lines are also detected. These UV results provide further support for the presence of a LLAGN in NGC 4579. On the other hand, Maoz et al. (1998) estimated the ionizing photon number by extrapolating the UV luminosity at 1300 Å toward higher energies and argued that the observed UV continuum is not sufficient to explain the H α luminosity. They also suggest that emission from AGNs is most prominent at energies higher than the UV. Measurements of an X-ray flux and continuum slope provide information on the ionization source in this LINER. In this paper, we report the detection of an iron K emission line centered at 6.7 keV and discuss the X-ray properties of the LLAGN in NGC 4579 and the origin of the iron emission line.

2. OBSERVATIONS

NGC 4579 was observed on 1995 June 25 with the *ASCA* satellite (Tanaka, Inoue, & Holt 1994). The solid-state imaging spectrometers (SIS0 and SIS1) were operated in the two CCD faint and bright mode. Effective exposure times were 32 and 3 ks for faint and bright mode data, respectively, after the standard data screening. As we can correct echo and dark frame errors, more reliable determination of absolute energy is possible for faint mode data than bright mode data (Otani & Dotani 1994). Since the SIS sensors were operated in faint mode during most of the observation time, we used only faint mode data for the following analyses. The gas imaging spectrometers (GIS2 and GIS3) were operated in the pulse-height nominal mode. We obtained a useful exposure of 31 ks after the standard data screening and the rejection of high background time intervals. X-ray light curves and spectra were extracted from circular regions centered on NGC 4579 with a radius of 4' for SIS and 6' for GIS. The spectra from SIS0 and SIS1 were added together after gain corrections. Spectra from GIS2 and GIS3 were also combined. Background data were accumulated from a source-free region in the same field. The mean counting rates of SIS and GIS were 0.15 counts s⁻¹ in 0.5–10 keV and 0.09 counts s⁻¹ in 0.7–10 keV per detector, respectively, after background subtraction. No significant variability was detected during the observation. A constant model fit to the light curve with a bin size of 5760 s (one orbit of the *ASCA* satellite) in the 2–10 keV band yields a

reduced χ^2 of 1.29 for 16 degrees of freedom (dof). The upper limit on the variability amplitude is 7% (root mean square) or 26% (peak-to-peak) for this light curve. Therefore, we summed all useful data together.

3. RESULTS

3.1. The X-Ray Image

NGC 4579 is detected at the position of the optical nucleus within position determination uncertainties, and the X-ray image looks pointlike. We compared X-ray images in the 0.5–2 and 2–10 keV band with the point-spread function (PSF) of the *ASCA* X-ray telescope plus SIS to evaluate the spatial extent. We fit the azimuthally averaged surface brightness profiles with those of a model PSF plus constant background, where we left two parameters free: the normalization of PSF and the background level. We obtained good fits with reduced chi-square $\chi^2_\nu = 0.64$ and 0.70 (11 dof) for the soft and the hard energy bands, respectively. Thus the images in these energy bands are consistent with a point source. In order to set an upper limit to the spatial extent, we fit the radial brightness profiles with those of a two-dimensional Gaussian convolved through the PSF (see Ptak 1997 for the technique). In this fitting, the free parameters are the Gaussian σ , the normalization of the Gaussian, and the background level. The upper limits of the Gaussian width are 0.25 for both the soft and the hard bands (0.25 corresponds to 1.2 kpc at 16.8 Mpc).

The fitted background level is ~ 2.5 times higher than that of the blank sky observations released by the NASA Guest Observer Facility in the 0.5–2 keV band, while the 2–10 keV background is consistent with the blank sky fields. NGC 4579 is located ~ 1.8 away from M87 in the Virgo Cluster of galaxies, and soft diffuse emission due to the intracluster gas is present in this region (Böhringer et al. 1994). Thus, the high background level in the soft band is most likely due to Virgo Cluster emission. In the soft-band image, no significant structure is seen.

3.2. The X-Ray Spectrum

The X-ray spectra obtained with the SIS and the GIS are shown in Figure 1. The X-ray spectra could not be fitted with simple power-law or thermal bremsstrahlung model, and residuals were clearly seen around 1 and 6.7 keV, which can be identified with iron L line complex and with an iron K emission line, respectively. An acceptable fit is obtained with the sum of a power law, a Raymond-Smith (R-S) thermal plasma model (Raymond & Smith 1977), and a Gaussian at 6.7 keV. In the fitting, the absorption column density is assumed to be the Galactic value (3.1×10^{20} cm⁻²; Murphy et al. 1996) for the R-S component and left free for the power-law component. The best-fit parameters of the X-ray continuum are summarized in Table 1, and the best-fit models are also shown in Figure 1 as a histogram.

TABLE 1
RESULTS OF SPECTRAL FITTING TO THE SIS AND GIS SPECTRA OF NGC 4579

Model	N_{H} (Galactic) (10^{20} cm ⁻²)	kT (keV)	Abundance (Soft Component) (solar)	N_{H} (10^{20} cm ⁻²)	Γ or kT (keV)	Abundance (Hard Component) (solar)	χ^2/dof
Raymond-Smith plus power law	3.1(f)	$0.90^{+0.11}_{-0.05}$	0.50(f)	4.1 ± 2.7	1.72 ± 0.05	...	192.4/201
Raymond-Smith plus Raymond-Smith	3.1(f)	$0.88^{+0.11}_{-0.05}$	0.50(f)	0(f)	$7.9^{+1.3}_{-0.9}$	$0.55^{+0.18}_{-0.16}$	198.2/204

NOTE.—An (f) in the table denotes a frozen parameter. The quoted errors are at the 90% confidence level for one interesting parameter.

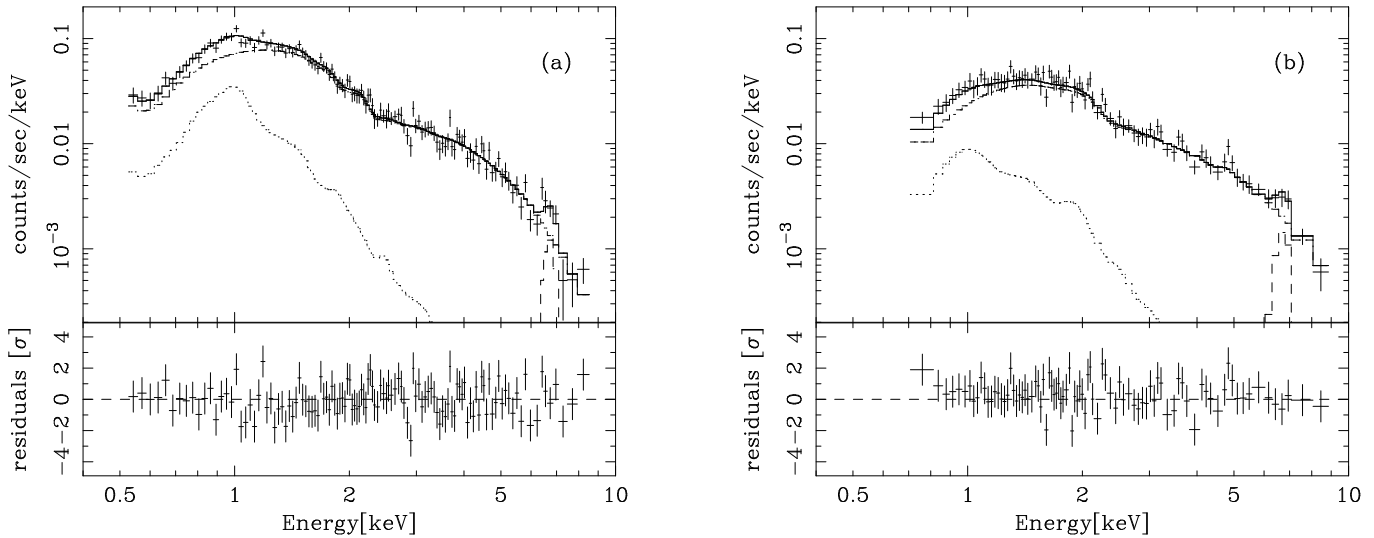


FIG. 1.—*ASCA* (a) SIS and (b) GIS spectra of NGC 4579. The best-fit model consists of an R-S thermal plasma, a power law, and a Gaussian and is shown as histograms. SIS and GIS data are plotted separately for clarity.

The photon index of the power-law component is 1.72 ± 0.05 (hereafter, quoted errors are 90% confidence for one interesting parameter), and the X-ray luminosity of this component is 1.5×10^{41} ergs s^{-1} in the 2–10 keV band. Although a small excess absorption of $N_{\text{H}} = (4 \pm 3) \times 10^{20}$ cm^{-2} is necessary to fit the data in addition to the Galactic absorption, N_{H} is still consistent with the Galactic value if the calibration uncertainties of the SIS at low energies are taken into account. Since the power-law component dominates the X-ray flux even in the soft energy band, the abundance of the metals in the R-S component is poorly constrained. Therefore, we fixed the abundance at 0.5 solar, which is typical for hot gas in spiral galaxies (e.g., Ptak 1997). Then the soft component is represented by the R-S model with $kT = 0.90_{-0.05}^{+0.11}$ keV. The addition of the R-S component to the power law plus Gaussian model improved the χ^2 significantly ($\Delta\chi^2 = 33.4$), and this decomposition of the spectrum is very similar to that of many other low-luminosity objects observed by *ASCA* (Serlemitsos, Ptak, & Yaqoob 1996). The X-ray luminosity of the R-S component is 1.2×10^{40} ergs s^{-1} in the 0.5–4 keV band. The luminosity of the R-S component depends on the assumed abundance value, and 0.88×10^{40} and 1.7×10^{40} ergs s^{-1} are obtained for assumed abundance values 1.0 and 0.1 solar, respectively. The hard-band spectrum can be also represented by an R-S thermal plasma with $kT = 7.9_{-0.9}^{+1.3}$ keV and an abundance of $0.55_{-0.16}^{+0.18}$ instead of a power law plus Gaussian model (Table 1).

An iron K line is clearly detected in the X-ray spectra: the addition of a Gaussian line improved χ^2 by 20.0 for three additional parameters (line center energy, line width, and normalization). Therefore, the iron line is statistically significant at greater than 99.9% confidence according to the *F*-test. The line center energy is $6.73_{-0.12}^{+0.13}$ keV (rest-frame), which is higher than the 6.4 keV typically observed from Seyfert 1 galaxies. The equivalent width is 490_{-190}^{+180} eV. The iron line profile is shown in Figure 2 as the ratio of the data to the best-fit continuum component of the above fits. Figure 3 shows the confidence contours for the line energy and the intensity. The best-fit energy agrees with He-like iron, and the 90% confidence range corresponds to the ion-

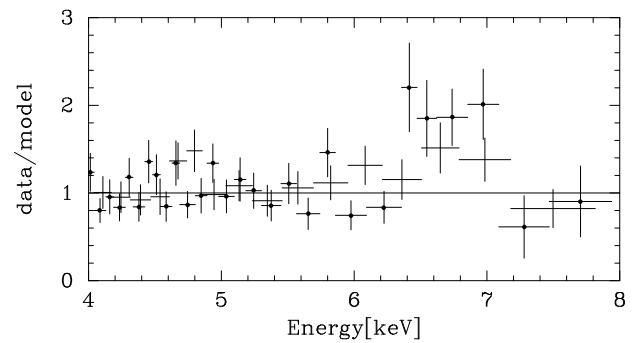


FIG. 2.—Data/model ratio for the best-fit continuum model around an iron K emission line. The crosses with and without filled circles represent SIS and GIS data, respectively. The energy scale is not redshift corrected.

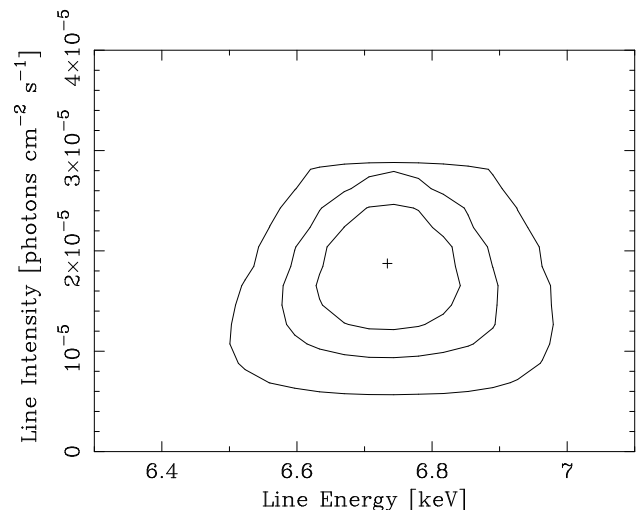


FIG. 3.—Confidence contours for the line energy and intensity. The energy scale is redshift corrected. The contours correspond to 68%, 90%, and 99% confidence level for two interesting parameters ($\Delta\chi^2 = 2.3, 4.6$, and 9.2, respectively).

TABLE 2
GAUSSIAN FITS TO THE IRON K LINE

Model	E_L [keV]	σ [keV]	EW [eV]	χ^2/dof
Narrow Gaussian	$6.82^{+0.10}_{-0.26}$	0(f)	360^{+175}_{-135}	195.5/202
Broad Gaussian	$6.73^{+0.13}_{-0.12}$	$0.17^{+0.11}_{-0.12}$	490^{+180}_{-190}	192.4/201
Three narrow Gaussians	6.4(f)	0(f)	110^{+130}_{-110}	192.6/201
	6.7(f)	0(f)	240^{+170}_{-160}	
	7.0(f)	0(f)	160^{+190}_{-160}	

NOTE.—An (f) in the table denotes a frozen parameter.

ization state from Fe xx to Fe xxv (He-like). A line center energy of 6.4 keV, which is expected from cold or low-ionization iron, is excluded at greater than the 99% confidence level. The confidence contours for the line width σ and the intensity are shown in Figure 4. The emission line is marginally broad. Although the best-fit width is $\sigma = 170$ eV, a narrow line cannot be excluded at 90% confidence level for two interesting parameters. If we fix the line width at $\sigma = 0$, a line center energy of $6.82^{+0.10}_{-0.26}$ keV and an equivalent width of 360^{+175}_{-135} eV are obtained.

A combination of multiple narrow lines instead of a single broad Gaussian also provides a good fit ($\chi^2_v = 0.958$ for 201 dof), where the line center energies are fixed at 6.4, 6.7, and 7.0 keV, which represent cold, He-like, and H-like iron, respectively. The obtained equivalent widths are 110^{+130}_{-110} , 240^{+170}_{-160} , and 160^{+190}_{-160} eV, respectively (Table 2). The 6.7 keV line is the dominant component in this model as well.

Many Seyfert 1 galaxies show broad iron lines with a significant red tail, and they are interpreted as originating from the inner part of a relativistic accretion disk (e.g., Tanaka et al. 1995). We examined the disk-line model by Fabian et al. (1989) instead of the Gaussian model. Since the statistics are limited, only two parameters, the inclination angle of the disk and the normalization, were left free. The inclination angle is defined such that $i = 0$ corresponds to a face-on disk. The line emissivity is assumed to be proportional to r^{-q} , and q is fixed at 2.5, which is the typical value for Seyfert 1 galaxies (Nandra et al. 1997a). The line

center energy is fixed at 6.4 or 6.7 keV. The inner radius of the line-emitting region was fixed at $6r_g$, where $r_g = GM/c^2$ is the gravitational radius. The outer radius is fixed at the χ^2 local minima for the fits, $16.6r_g$ and $10.5r_g$ for the 6.4 and 6.7 keV cases, respectively. The disk-line model fits provided worse reduced χ^2 values ($\Delta\chi^2 \sim 8$) than the Gaussian modeling of the line. The best-fit parameters are summarized in Table 3. Although the fit is acceptable, systematic positive residuals are seen around 6.7 keV. This is probably due to absence of significant red asymmetry in the observed profile. The obtained equivalent width, ~ 900 eV, is extremely large compared to the value expected from a X-ray irradiated disk (e.g., George & Fabian 1991) and observed in Seyfert 1 galaxies (Nandra et al. 1997a).

4. DISCUSSION

4.1. X-Ray Emission from a Low-Luminosity AGN

We obtained X-ray images and spectra in the 0.5–10 keV band, and a pointlike X-ray source with a photon index of $\Gamma = 1.72 \pm 0.05$ is detected. An iron line is also detected at 6.7 keV. In the soft energy band, a broad line feature identified with iron-L line complex indicates the presence of thin thermal plasmas of temperature $kT \sim 0.9$ keV.

The X-ray luminosity (1.5×10^{41} ergs s^{-1} in 2–10 keV) is 1–3 orders of magnitude smaller than typical Seyfert galaxies and falls in the classes of LINERs and “low-luminosity” Seyfert galaxies (Serlemitsos et al. 1996; Iyomoto et al. 1996; Ishisaki et al. 1996; Terashima et al. 1998b). In normal spiral galaxies, the X-ray emission is dominated by discrete sources, specifically low-mass X-ray binaries (LMXBs) (e.g., Fabbiano 1989; Makishima et al. 1989). The X-ray luminosity from LMXBs is roughly proportional to the B-band luminosity L_B , and their X-ray spectra can be approximated by a thermal bremsstrahlung of a temperature of several keV. The ASCA X-ray spectrum of NGC 4579 is also fitted by $kT \sim 8$ keV thermal plasma model. However, the strong iron line at 6.7 keV is not compatible with the X-ray spectra of LMXBs, since the equivalent widths of iron emission lines from LMXBs are small (several tens of electron volts) (Hirano et al. 1987). Additionally, the L_X/L_B value 1.3×10^{-3} is more than an order

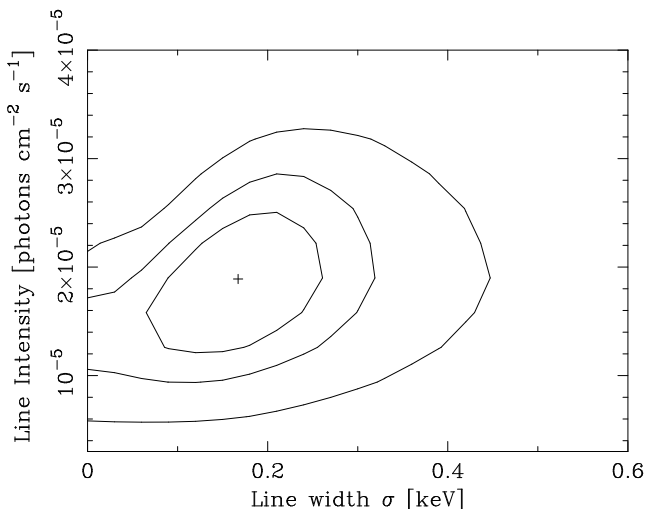


FIG. 4.—Confidence contours for the line width (Gaussian σ) and intensity. The contours correspond to 68%, 90%, and 99% confidence level for two interesting parameters.

TABLE 3
DISK-LINE MODEL FITS TO THE IRON K LINE

E_L (keV)	R_{in} (R_g)	R_{out} (R_g)	i (deg)	EW (eV)	χ^2/dof
6.4(f).....	6(f)	16.6(f)	42 ± 4	880^{+570}_{-360}	200.7/202
6.7(f).....	6(f)	10.5(f)	36 ± 3	920^{+530}_{-320}	201.5/202

NOTE.—An (f) in the table denotes a frozen parameter.

of magnitude higher than normal spiral galaxies (e.g., $L_X/L_B = 3.5 \times 10^{-5}$ for M31; Makishima et al. 1989). Additionally, an upper limit on the size of an archival *ROSAT* PSPC image is $14''$ (Gaussian σ), which corresponds to 1.1 kpc at 16.8 Mpc. This upper limit is significantly lower than the size of the galaxy. Therefore, we conclude that contribution from LMXBs to the X-ray emission of NGC 4579 is negligible.

Hot plasmas with temperatures on the order of ~ 10 keV are present in the Galactic center region, and their X-ray spectra show prominent, ionized iron K emission (e.g., Koyama et al. 1996). The X-ray spectral shape of NGC 4579 in the hard X-ray band is similar to such hot gas. However, the X-ray luminosity of NGC 4579 is 3 orders of magnitude higher than the Galactic ridge emission ($L_X \sim 2 \times 10^{38}$ ergs s^{-1} ; Kaneda et al. 1997; Yamasaki 1996; Warwick et al. 1985). Starburst galaxies also show a hard spectral component with a temperature of ~ 10 keV, and their X-ray luminosities are around 10^{40} ergs s^{-1} (e.g., 3.4×10^{40} ergs s^{-1} in 2–10 keV for M82; Ptak et al. 1997). However, the starburst activity in NGC 4579 is weaker than that in M82, since the far-infrared luminosity of NGC 4579 is about an order of magnitude lower than that of M82. Furthermore, starburst galaxies show weak or no iron emission, contrary to NGC 4579. Therefore, hot plasma is unlikely as the origin of the hard component and the iron emission line in NGC 4579, and we conclude that the AGN emission dominates the *ASCA* spectra and that the contribution of other components, such as a hot gas, is small, if existent.

We note that errors in background subtraction of the Virgo Cluster hot gas do not affect the detection of the iron emission line at 6.7 keV, since the cluster gas is very dim in this region and the temperature is low ($kT \sim 2$ keV; Matsumoto 1998; Böhringer et al. 1994). Actually, no significant iron emission is detected from the GIS field around NGC 4579.

If the primary ionizing mechanism of LINER optical emission lines in this galaxy is photoionization by a LLAGN, $L_X/L_{H\alpha}$ might be expected to be similar to Seyfert 1 galaxies, for which there is a good positive correlation between L_X and $L_{H\alpha}$ (e.g., Ward et al. 1988; Koratkar et al. 1995; Serlemitsos et al. 1996). Using the $H\alpha$ luminosity of broad plus narrow component $L_{H\alpha} = 5.9 \times 10^{39}$ ergs s^{-1} (Ho et al. 1997b) and the observed X-ray luminosity in the 2–10 keV band, we obtain $L_X/L_{H\alpha} \approx 26$ for NGC 4579. This value is in excellent agreement with those of Seyfert 1 galaxies (Ward et al. 1988) and strongly supports a low-luminosity AGN as the ionizing source of the LINER in NGC 4579.

Less luminous Seyfert 1 galaxies tend to show rapid and large-amplitude variability (Mushotzky, Done, & Pounds 1993 and references therein). However, NGC 4579 shows no significant short-term variability. Lack of variability on short timescales seems to be a common property of LLAGNs (Mushotzky 1992; Petre et al. 1993)—for example, the LLAGN in NGC 1097 (Iyomoto et al. 1996) and NGC 3998 (Awaki et al. 1991) also show no significant variability on timescales less than a day. Direct comparison of *ROSAT* PSPC and *ASCA* flux in the 0.5–2 keV band shows a factor of 2 increase in ~ 3.5 yr.

The X-ray spectral slope $\Gamma = 1.72 \pm 0.05$ is identical to the average value found for hard X-ray selected Seyfert 1 galaxies (Mushotzky et al. 1993), but the luminosity is lower than that of any Seyfert 1 galaxy except NGC 4051. Based

on the full width at zero intensity of a broad emission line and an estimate of the size of the broad-line region, the mass of the central black hole is roughly estimated to be $M_* \sim 4 \times 10^6 M_\odot$. Then the Eddington ratio L/L_{Edd} is $\sim 10^{-3}$ for the observed luminosity of $\sim 5 \times 10^{41}$ ergs s^{-1} (Barth et al. 1996), although their black hole mass estimation is crude. Therefore, the X-ray spectral slope does not seem to be drastically changed even at a very low Eddington ratio. This is also true for M81, for which L/L_{Edd} is estimated to be $\sim (2-10) \times 10^{-4}$ (Ho, Filippenko, & Sargent 1996) and the photon index is 1.85 ± 0.04 (Ishisaki et al. 1996).

Soft thermal emission of $kT \sim 0.5 - 1$ keV is often observed from LLAGNs (Terashima 1997; Ptak 1997; Serlemitsos et al. 1996). In some cases, such emission is associated with starburst activity (e.g., Iyomoto et al. 1996; Terashima et al. 1998a). Since the far-infrared luminosity of NGC 4579 is 1.5×10^{43} ergs s^{-1} , some star formation activity may be present, which may explain the thermal emission. The soft thermal X-ray-to-far-infrared luminosity ratio of $L_X/L_{\text{FIR}} = 6 \times 10^{-4}$ to 1.1×10^{-3} is consistent with starburst galaxies (e.g., David, Jones, & Forman 1992) within the scatter.

4.2. Iron K Line

A marginally broad ($\sigma \approx 0.17$ keV) iron emission line is clearly detected at $6.73_{-0.12}^{+0.13}$ keV, and the equivalent width is 490_{-190}^{+180} eV for the broad Gaussian model fit. The line center energy is significantly higher than 6.4 keV, which is typically observed from Seyfert 1 galaxies, and it is consistent with He-like iron. A similar broad iron line centered at ~ 6.7 keV is detected from the low-luminosity Seyfert galaxy M81 (Ishisaki et al. 1996; Serlemitsos et al. 1996). The line can also be represented by line blending of neutral, He-like, and H-like iron, dominated by He-like iron. The disk-line profile (Fabian et al. 1989) is probably inconsistent with the data for 6.4 or 6.7 keV intrinsic line energy for the following reasons. The χ^2 value is worse than a single broad Gaussian fit, and systematic residuals remain in the disk-line fit, since a significant red tail is not clearly seen in the data. Furthermore, the disk-line model provides a very large equivalent width, ~ 900 eV, which is about 4 times larger than the results of the disk-line fit to Seyfert 1 galaxies [$\langle \text{EW} \rangle = (230 \pm 60)$ eV; Nandra et al. 1997a]. Therefore, our data prefer a symmetric Gaussian-shape profile with an intrinsic line center energy of 6.7 keV (He-like) rather than 6.4 keV (less than Fe xvii). Thus, the ionization state of the iron line emitter may be different from that of higher luminosity Seyfert 1 galaxies in at least some LLAGNs (NGC 4579 and M81).

Strong ionized iron emission lines are observed in heavily obscured Seyfert 2 galaxies (NGC 1068: Ueno et al. 1994; Iwasawa, Fabian, & Matt 1997; NGC 1365: Iyomoto et al. 1997; see also Turner et al. 1997a, 1997b). In these objects, continuum emission from the nucleus is completely blocked, and only scattered radiation is observed. Ionized iron lines are interpreted as originating from a photoionized scattering medium. If the continuum of NGC 4579 is scattered radiation, then the observed X-ray luminosity is only a fraction of its intrinsic luminosity. Since the scattering fraction is typically less than 10% for Seyfert 2 galaxies (Ueno 1995), $L_X/L_{[\text{O III}]}$ should be less than 10% of those of Seyfert 1 galaxies, as is the case for NGC 1068 (Mulchaey et al. 1994). However, the observed X-ray-to-[O III] $\lambda 5007$ luminosity ratio $L_X/L_{[\text{O III}]}$ is very similar to Seyfert 1 gal-

axies. Therefore, the observed X-ray continuum is not likely to be due to a scattered component, and the observed iron line should be emitted from the matter close to the nucleus in order to be ionized and/or broadened due to the Doppler effect.

If the iron line is emitted by an accretion disk, a line profile with significant red tail is expected (Fabian et al. 1989). On the other hand, the observed profile seems to be symmetric in shape, although the statistics are limited. Broad lines with weaker red tails than Seyfert 1 galaxies are observed in AGNs with much higher luminosity: $L_X > 10^{44}$ ergs s^{-1} (Nandra et al. 1997b). If the innermost part of the accretion disk is almost fully ionized, the red component is expected to be very weak or absent. Thus, the observed profile is consistent with the interpretation that the observed iron K emission is from an ionized disk.

The obtained equivalent width (~ 500 eV for the Gaussian model) is rather large compared to that seen in most Seyfert 1 galaxies. If the disk is highly ionized, the fluorescence yield of iron increases, and absorption by lighter elements decreases as light elements are almost completely ionized. In such a situation, the equivalent width of an iron line can increase by a factor of 2 (Matt et al. 1993; Życki & Czerny 1994). Therefore, the large equivalent width is also naturally explained by an ionization effect.

The ionization state of photoionized matter is determined by an ionization parameter $\xi = L/nR^2$ (Kallman & MacCray 1982), where L , n , and R are the luminosity of ionizing photons, the number density of photoionized matter, and the distance from light source to photoionized matter, respectively. The X-ray luminosity of NGC 4579 is only 1.5×10^{41} ergs s^{-1} , which is 1–3 orders of magnitude smaller than that for Seyfert 1 galaxies, and the X-ray luminosity of M81, from which an iron line centered at ~ 6.7 keV is detected, is even lower ($\sim 2 \times 10^{40}$ ergs s^{-1}). In order to photoionize iron atoms to be He-like, ξ should be at least ~ 500 , while $\xi < 100$ is required for less ionized species (less than Fe xvii), which is probably appropriate for usual Seyfert 1 galaxies. Therefore, nR^2 in the iron line-emitting region should be more than 2 orders of magnitude smaller than that of luminous Seyfert 1 galaxies. An expected ionization parameter under an assumption of standard α disk is calculated by Matt et al. (1993). According to their results, the ionization parameter has a strong dependence on the mass accretion rate $\xi \propto \dot{m}^3$ (eqs. [5] and [6] in Matt et al. 1993), where \dot{m} is denoted in units of the critical accretion rate $\dot{m} = L/L_{\text{Edd}}$. In order to ionize iron to be He-like, \dot{m} should be at least 0.2 (Figs. 2 and 5 in Matt et al. 1993). However, the order-of-magnitude estimate of the central black hole mass by Barth et al. (1996) combined with the observed luminosity gives a significantly smaller value of $\dot{m} \sim 1 \times 10^{-3}$. Thus we cannot explain the very low lumi-

nosity and the ionized iron line at the same time in the standard disk model. This may suggest that the accretion process in AGNs is different in very low luminosity situations with very small \dot{m} .

An advection-dominated accretion flow (ADAF) model is proposed for AGNs specifically for objects radiating at very low Eddington ratios (e.g., $\dot{m} \sim 10^{-4}$ for NGC 4258; Lasota et al. 1996). In the model by Lasota et al. (1996), a standard disk is assumed outside of r_{in} and an ADAF is assumed inside of r_{in} . In an ADAF, accreting matter is heated up to very high temperatures ($T_i \sim 10^{12}$ K, $T_e \sim 10^9$ K). However, our detection of an iron line indicates the presence of highly ionized (but not fully ionized) matter surrounding a large solid angle viewed from the light source. This means that r_{in} should be small, and a geometrically thin disk is appropriate. Therefore, the iron line in NGC 4579 cannot be explained solely by an ADAF model, and the real situation in NGC 4579 may correspond to a condition near the transition from the α disk to an ADAF.

Future sophisticated modeling of accretion in LLAGNs and calculations of expected iron emission as well as precise measurements of an iron K line and mass determination by the *HST* Space Telescope Imaging Spectrograph will be important in helping us understand physical processes in extremely low-luminosity AGNs.

5. SUMMARY

We observed the LINER NGC 4579 with *ASCA* and detected X-ray emission with a luminosity of 1.5×10^{41} ergs s^{-1} probably from a LLAGN. The X-ray spectral slope ($\Gamma = 1.72 \pm 0.05$) is quite similar to Seyfert 1 galaxies. Iron K emission is detected at 6.7 keV, which is consistent with He-like iron, with an equivalent width of 500 eV. Although the statistics are limited, the observed iron line profile shows no significant red tail, and a symmetrically shaped He-like iron line is preferred rather than a blueshifted component of the disk-line profile from neutral or low-ionization iron, as seen in Seyfert 1 galaxies. The observed center energy, profile, and equivalent width of iron emission are well explained in terms of an ionized disk origin. However, the ionization parameter cannot be large enough to ionize the disk with the inferred low Eddington ratio (Matt et al. 1993). The detection of iron emission indicates that a large solid angle seen from the X-ray source is surrounded by ionized material. This is inconsistent with an advection-dominated accretion flow model for LLAGNs (Lasota et al. 1996).

The authors are grateful to all the *ASCA* team members. Y. T. and K. M. thank the Japan Society for the Promotion of Science for support.

REFERENCES

- Awaki, H., Koyama, K., Kunieda, H., Takano, S., Tawara, Y., & Ohashi, T. 1991, *ApJ*, 366, 88
 Barth, A., Reichert, G. A., Filippenko, A. V., Ho, L. C., Shields, J. C., Mushotzky, R. F., & Puchnarewicz, E. M. 1996, *AJ*, 112, 1829
 Böhringer, H., Briel, U. G., Schwarz, R. A., Voges, W., Hartner, G., & Trümper, T. 1994, *Nature*, 368, 828
 David, L. P., Jones, C., & Forman, W. 1992, *ApJ*, 388, 82
 Fabbiano, G. 1989, *ARA&A*, 27, 87
 Fabbiano, G., Kim, D.-W., & Trinchieri, G. 1992, *ApJS*, 80, 531
 Fabian, A. C., Rees, M. J., Stella, L., & White, N. E. 1989, *MNRAS*, 238, 729
 George, I. M., & Fabian, A. C. 1991, *MNRAS*, 249, 352
 Halpern, J. P., & Steiner, J. E. 1983, *ApJ*, 269, L37
 Heckman, T. M. 1980, *A&A*, 87, 152
 Hirano, T., Hayakawa, S., Nagase, F., Masai, K., & Mitsuda, K. 1987, *PASJ*, 39, 619
 Ho, L. C., Filippenko, A. V., & Sargent, W. L. W. 1996, *ApJ*, 462, 183
 ———. 1997a, *ApJS*, 112, 315
 Ho, L. C., Filippenko, A. V., Sargent, W. L. W., & Peng, C. Y. 1997b, *ApJS*, 112, 391
 Hummel, E., van der Hulst, J. M., Keel, W. C., & Kennicutt, R. C., Jr. 1987, *A&AS*, 70, 517
 Ishisaki, Y., et al. 1996, *PASJ*, 48, 237
 Iwasawa, K., Fabian, A. C., & Matt, G. 1997, *MNRAS*, 289, 443
 Iwasawa, K., Fabian, A. C., Mushotzky, R. F., Brandt, W. N., Awaki, H., & Kunieda, H. 1996, *MNRAS*, 279, 873

- Iyomoto, N., Makishima, K., Fukazawa, Y., Tashiro, M., & Ishisaki, Y. 1997, *PASJ*, 49, 425
- Iyomoto, N., Makishima, K., Fukazawa, Y., Tashiro, M., Ishisaki, Y., Nakai, N., & Taniguchi, Y. 1996, *PASJ*, 48, 231
- Kallman, T. R., & MacCray, R. 1982, *ApJS*, 50, 263
- Kaneda, H., Makishima, K., Yamauchi, S., Koyama, K., Matsuzaki, K., & Yamasaki, N. Y. 1997, *ApJ*, 491, 638
- Keel, W. C. 1983, *ApJ*, 269, 466
- Kii, T., et al. 1991, *ApJ*, 367, 455
- Koratkar, A., Deustua, S. E., Heckman, T., Filippenko, A. V., Ho, L. C., & Rao, M. 1995, *ApJ*, 440, 132
- Koyama, K., Maeda, Y., Sonobe, T., Takeshima, T., Tanaka, Y., & Yamauchi, S. 1996, *PASJ*, 48, 249
- Lasota, J. P., Abramowicz, M. A., Chen, X., Krolik, J., Narayan, R., & Yi, I. 1996, *ApJ*, 462, 142
- Makishima, K., et al. 1989, *PASJ*, 41, 697
- Maoz, D., Filippenko, A. V., Ho, L. C., Rix, H.-W., Bahcall, J. N., Schneider, D. P., & Macchetto, F. D. 1995, *ApJ*, 440, 91
- Maoz, D., Koratkar, A., Shields, J. C., Ho, L. C., & Filippenko, A. V. 1998, *AJ*, in press
- Matsumoto, H. 1998, Ph.D. thesis, Kyoto Univ.
- Matt, G., Fabian, A. C., & Ross, R. R. 1993, *MNRAS*, 262, 179
- Mulchaey, J. S., et al. 1994, *ApJ*, 436, 586
- Murphy, E. M., Lockman, F. J., Laor, A., & Elvis, M. 1996, *ApJS*, 105, 369
- Mushotzky, R. F. 1992, in *The Nearest Active Galaxies*, ed. H. Netzer & J. Beckman (Madrid: CSIC)
- Mushotzky, R. F., Done, C., & Pounds, K. A. 1993, *AR&A*, 31, 717
- Nandra, K., George, I. M., Mushotzky, R. F., Turner, T. J., & Yaqoob, T. 1997a, *ApJ*, 477, 602
- . 1997b, *ApJ*, 488, L91
- Nandra, K., George, I. M., Turner, T. J., & Fukazawa, Y. 1996, *ApJ*, 464, 165
- Otani, C., & Dotani, T. 1994, *ASCA Newslett.*, 2, 25
- Petre, R., Mushotzky, R. F., Serlemitsos, P. J., Jahoda, K., & Marshall, F. E. 1993, *ApJ*, 418, 644
- Ptak, A. 1997, Ph.D. thesis, Univ. Maryland
- Ptak, A., Serlemitsos, P., Yaqoob, T., Mushotzky, R., & Tsuru, T. 1997, *AJ*, 113, 1286
- Raymond, J. C., & Smith, B. W. 1977, *ApJS*, 35, 419
- Serlemitsos, P. J., Ptak, A., & Yaqoob, T. 1996, in *The Physics of LINERs in View of Recent Observations*, ed. M. Eracleous (San Francisco: ASP), 70
- Stauffer, J. R. 1982, *ApJ*, 262, 66
- Tanaka, Y., Inoue, H., & Holt, S. S. 1994, *PASJ*, 46, L37
- Tanaka, Y., et al. 1995, *Nature*, 375, 659
- Terashima, Y. 1997, Ph.D. thesis, Nagoya Univ.
- Terashima, Y., Ptak, A., Fujimoto, R., Itoh, M., Kunieda, H., Makishima, K., & Serlemitsos, P. J. 1998a, *ApJ*, 496, 210
- Terashima, Y., et al. 1998b, *PASJ*, submitted
- Tully, R. B. 1988, *Nearby Galaxies Catalog* (Cambridge: Cambridge Univ. Press)
- Turner, T. J., George, I. M., Nandra, K., & Mushotzky, R. F. 1997a, *ApJS*, 113, 23
- . 1997b, *ApJ*, 488, 164
- Ueno, S. 1995, Ph.D. thesis, Kyoto Univ.
- Ueno, S., Mushotzky, R. F., Koyama, K., Iwasawa, K., Awaki, H., & Hayashi, I. 1994, *PASJ*, 46, L71
- Warwick, R. S., Turner, M. J. L., Watson, M. G., & Willingale, R. 1985, *Nature*, 317, 218
- Yamasaki, N. Y. 1996, Ph.D. thesis, Univ. Tokyo
- Yamashita, A., et al. 1997, *ApJ*, 486, 763
- Ward, M. J., Done, C., Fabian, A. C., Tennant, A. F., & Shafer, R. A. 1988, *ApJ*, 324, 767
- Życki, P. T., & Czerny, B. 1994, *MNRAS*, 266, 653